AMERICAN SOCIETY FOR MICROBIOLOGY | Applied and Environmental Microbiology

Comparison of UV-Induced Inactivation and RNA Damage in MS2 Phage across the Germicidal UV Spectrum

Sara E. Beck,[a]* Roberto A. Rodriguez,[a]* Michael A. Hawkins,[a] Thomas M. Hargy,[b]* Thomas C. Larason,[c] Karl G. Linden[a]

Department of Civil, Environmental, and Architectural Engineering, University of Colorado, Boulder, Colorado, USA[a]; Tetra Tech, Saint Albans, Vermont, USA[b]; National Institute of Standards and Technology, Gaithersburg, Maryland, USA[c]

Polychromatic UV irradiation is a common method of pathogen inactivation in the water treatment industry. To improve its disinfection efficacy, more information on the mechanisms of UV inactivation on microorganisms at wavelengths throughout the germicidal UV spectrum, particularly at below 240 nm, is necessary. This work examined UV inactivation of bacteriophage MS2, a common surrogate for enteric pathogens, as a function of wavelength. The bacteriophage was exposed to monochromatic UV irradiation from a tunable laser at wavelengths of between 210 nm and 290 nm. To evaluate the mechanisms of UV inactivation throughout this wavelength range, RT-qPCR (reverse transcription-quantitative PCR) was performed to measure genomic damage for comparison with genomic damage at 253.7 nm. The results indicate that the rates of RNA damage closely mirror the loss of viral infectivity across the germicidal UV spectrum. This demonstrates that genomic damage is the dominant cause of MS2 inactivation from exposure to germicidal UV irradiation. These findings contrast those for adenovirus, for which MS2 is used as a viral surrogate for validating polychromatic UV reactors.

UV irradiation is a common method of disinfection in the water treatment industry. UV light induces damage to the genomes of bacteria, protozoa, and viruses, breaking bonds and forming photodimeric lesions in nucleic acids, DNA, and RNA (1, 2). These lesions prevent both transcription and replication and ultimately lead to inactivation of the microorganisms (3, 4). Direct UV damage to nucleic acids occurs at the wavelengths absorbed by DNA and RNA, in the germicidal UV region between 200 and 300 nm (5, 6). In this wavelength range, however, UV light also damages other cellular and viral components, causing, for example, photochemical reactions in proteins and enzymes (7, 8). For this reason, UV sources that emit polychromatic light, across the germicidal UV spectrum, are considered more effective at inactivating certain pathogens than sources that emit monochromatic light at 253.7 nm (9–12). As polychromatic sources become more common, more research is being undertaken to understand the mechanisms of inactivation occurring in pathogens exposed to polychromatic UV irradiation.

Male-specific (MS2) coliphage is a single-stranded RNA virus. It infects strains of *Escherichia coli* that produce F^+ pili, which serve as viral receptors. The virion consists of a short single-stranded RNA genome (3,569 bases) surrounded by an icosahedral protein capsid, 27 nm in diameter (13). MS2 is commonly used in the water treatment industry as a surrogate for enteroviruses because of its similar size, shape, and genome composition (9, 14). It serves as a biodosimeter for UV disinfection studies (15) and for UV reactor validation in North America (14, 16). For reactor validation, MS2 is also used as a surrogate for *Cryptosporidium* and adenovirus, despite the differences in UV sensitivity and spectral sensitivity between these microorganisms. Recent interest has grown regarding microbial and viral sensitivity to UV irradiation at wavelengths below 240 nm. Irradiation from some newer medium-pressure (MP) mercury vapor lamps is richer at wavelengths below 240 nm. Furthermore, type 219 quartz sleeves, which were commonly used in practice and are standard in European applications of MP UV, absorb most of the low-wavelength light. Recently, however, vendors have been replacing type 219 sleeves with type 214 sleeves, which transmit 51% of the light at 200 nm, or with synthetic quartz sleeves, which transmit 89% of the light at 200 nm (H. Wright, M. Heath, and J. Bandy, presented at the 2nd Joint IOA/IUVA World Congress, Paris, France, 2011).

The use of lamp systems with type 214 and synthetic quartz sleeves with MS2 as a validation test organism for pathogens such as *Cryptosporidium* can overpredict the UV dose delivered, raising a potential public health concern (Wright et al., presented at the 2nd Joint IOA/IUVA World Congress). Additionally, for adenovirus, it was shown that UV light at wavelengths below 240 nm induces damage to a viral component other than nucleic acid, contributing significantly to its loss of infectivity (12). Knowledge about inactivation at the lower UV wavelengths prompted the desire to understand more about the inactivation mechanisms involved at these wavelengths. It was particularly important to evaluate MS2, given its importance to the water treatment industry and its use as a surrogate for both *Cryptosporidium* and adenovirus.

Many studies have compared the spectral sensitivity or action spectrum of an organism or virus to the absorbance of its DNA

Received 31 August 2015 **Accepted** 13 December 2015

Accepted manuscript posted online 28 December 2015

Citation Beck SE, Rodriguez RA, Hawkins MA, Hargy TM, Larason TC, Linden KG. 2016. Comparison of UV-induced inactivation and RNA damage in MS2 phage across the germicidal UV spectrum. Appl Environ Microbiol 82:1468–1474. doi:10.1128/AEM.02773-15.

Editor: C. M. Dozois, INRS—Institute Armand-Frappier

Address correspondence to Karl G. Linden, karl.linden@colorado.edu.

* Present address: Sara E. Beck, School of Environment, Resources, and Development, Asian Institute of Technology, Pathumthani, Thailand; Roberto A. Rodriguez, Environmental and Occupational Health Sciences, School of Public Health, El Paso Regional Campus, University of Texas Health Science Center at Houston, El Paso, Texas, USA; Thomas M. Hargy, Corona Environmental Consulting, Fairfax, Vermont, USA.

TABLE 1 Primers and probe used for reverse transcription and quantitative PCR

Purpose and primer or probe	Sequence[a]	Genome region (positions)	Fragment size (no. of bases)[a]	Reference
Reverse transcription				
Reverse primer 3424	TCT TTC GAG CAC ACC CAC C	3405–3424	2,169	24
Reverse primer 2440	TCT ATA CCA ACG GAT TTG AGC C	2418–2440	1,185	This work
Quantitative PCR				
Forward primer	TCG ATG GTC CAT ACC TTA GAT GC	1255–1277		26
Reverse primer	ACC CCG TTA GCG AAG TTG CT	1404–1423		26
Probe	5′–FAM–TC TCG TCG ACA ATG GC–3′–BHQ-2[b]	1362–1375		26

[a] Size of the RNA analyzed using this reverse primer for reverse transcription and in reference to the site used for the real-time PCR assay.
[b] FAM, 6-carboxyfluorescein; BHQ-2, black hole quencher 2 dye.

(15, 17–19; M. Stefan, C. Odegaard, B. Petri, M. Rowntree, and L. Sealey, presented at the 1st Joint IOA/IUVA World Congress, Los Angeles, CA, 2007). Fewer studies have measured the damage that occurs within DNA or RNA as a result of the absorbance of UV irradiation (6, 12). This research analyzes the wavelength-specific effects of UV light on the bacteriophage MS2 by analyzing damage to its viral RNA. RNA differs from DNA in composition primarily by the presence of uracil nucleotides instead of thymine. UV irradiation forms several RNA photoproducts, primarily from adjacent pyrimidine nucleotides, such as uracil dimers (20, 21), as well as RNA-protein cross-links (22). These lesions, which inhibit RNA synthesis primarily through the formation of 6-4 photoproducts (23), also block the reverse transcriptase enzyme (4) from transcribing strands of cDNA, making the reverse transcription-quantitative PCR (RT-qPCR) assay suitable for detecting damage to the viral RNA. Previous research used reverse transcription-quantitative PCR to confirm that after exposure to UV light at 253.7 nm, the loss of viral infectivity of MS2 was due to RNA damage (24). This research examined the role of other wavelengths emitted by polychromatic UV systems to determine whether those findings extended across the germicidal UV range. This work complements previous work by those authors on viral DNA damage. It provides a perspective on the differences between adenovirus, a UV-resistant pathogen, and its commonly used MS2 surrogate across the germicidal UV range as well as the subsequent implications for UV disinfection practice.

MATERIALS AND METHODS

UV irradiations. UV irradiations of MS2 coliphage suspended in phosphate-buffered saline (PBS) were conducted by using an NT242 series Ekspla tunable laser provided by the National Institute of Standards and Technology (NIST) (Gaithersburg, MD). As described previously (12), the tunable laser provided precise UV irradiations (bandwidth of <0.1 nm) at wavelengths of between 210 nm and 290 nm at ~10-nm intervals. At each wavelength, four collimated beam exposures were conducted to generate a dose-response curve demonstrating up to 3-log inactivation of MS2 coliphage. The experiments were conducted twice, generating two dose-response curves. However, UV doses varied between the two trials; therefore, each data point represents one measurement. Irradiance was measured at the water surface by a photodiode detector (IRD SXUV 100; Opto Diode Corporation, Thousand Oaks, CA) and precision aperture (SK030483-1073; Buckbee Mears, Cortland, NY), both supplied by the NIST.

Average UV doses were determined as described previously by Bolton and Linden (25), adjusting for reflection off the water surface, UV absorption (measured by a Spectronic Genesys 10S UV-Vis spectrophotometer [Thermo Electron Scientific Instruments Corp., Madison, WI]), depth of the water sample, and the nonuniform distribution of light across the sample surface. Quiescently stirred samples of 5 ml (0.6-cm depth) were irradiated in 3.5-cm-diameter petri dishes. Laser irradiance varied with each wavelength examined between 11.4 $\mu W/cm^2$ and 221 $\mu W/cm^2$, and UV doses ranged from 4 mJ/cm^2 to 160 mJ/cm^2, depending on the wavelength tested. Beam divergence from the laser diffuser was assumed to be negligible but was measured and accounted for in the mercury lamp irradiation experiments described below.

Immediately after exposure, the irradiated samples were assayed for phage infectivity, and the remainders were stored at −80°C. An aliquot of each sample from the −80°C freezer was shipped to the University of Colorado—Boulder for molecular analysis.

Reverse transcription-quantitative PCR assay. The two-step RT-qPCR method detects UV damage in large fragments of the MS2 genome. It was adapted from methods described previously by Simonet and Gantzer (24), using a primer set for real-time PCR described previously (26) (Table 1).

Viral RNA was extracted by using a QIAamp viral RNA kit (Qiagen, Valencia, CA) according to the manufacturer's instructions and stored at −20°C. The reverse transcription step consisted of the use of 2 μl of the reverse primer (25 μM) for each 10-μl sample of extracted RNA. The sample was heated at 70°C for 5 min to anneal the primers and then rapidly chilled on ice for 1 min. The analysis was conducted with two separate reverse primers to analyze the MS2 dose response, resulting in two different lengths of cDNA produced. Reverse primers 3424 and 2440 (Table 1) were used to analyze fragments of 2,169 and 1,185 bases, respectively. The primer for reverse transcription (primer 3424) was described previously for MS2 inactivation experiments and was selected as a reference for comparison to previous work on viral RNA damage (24). A second primer (primer 2440) was designed in the present study to provide a smaller fragment for better resolution for the detection of RNA damage at higher UV doses.

The samples described above were combined with a reverse transcription mix containing 1 μl of Improm II reverse transcription enzyme (200 U/μl; Promega, Madison, WI), 5 μl of its 5× reaction buffer, 3 μl of 25 mM $MgCl_2$ (Promega), 1 μl of deoxynucleotide triphosphate (dNTP) nucleotide mix (10 mM; Fermentas, Thermo Fisher Scientific, Waltham, MA), 0.5 μl of RNase inhibitor (RNasin, 20 to 40 U/μl; Promega), and nuclease-free water for a total volume of 25 μl per sample. The mixture was heated to 42°C for 60 min for cDNA transcription, followed by chilling on ice.

qPCR was used to quantify the RT products. A 2-μl volume of the cDNA was combined with a reaction mix containing 12.5 μl of QuantiTect Probe PCR master mix (Qiagen), 0.5 μl of 7.5 mM forward and reverse primers, 0.5 μl of 7.5 mM probe, and nuclease-free water for a total reaction mixture volume of 25 μl. The primers and probes, synthesized by Integrated DNA Technologies (Coralville, IA), are given in Table 1.

The qPCR assays were performed in duplicate by using an MJ MiniOpticon real-time PCR machine (Bio-Rad, Hercules, CA). In the thermocycle program, the samples were heated to 94°C for 10 min before repeating 50 times a cycle of 10 s at 94°C to denature the DNA strands, followed by 1 min at 60°C to anneal the primer and probe and synthesize new DNA. The fluorescence signal was read at the end of each cycle.

UV absorption of RNA. Viral RNA from the MS2 coliphage stock (10^8 PFU/ml) was extracted as described above. The UV absorption from 220 nm to 300 nm was measured relative to the absorption of the elution buffer by using a UV spectrophotometer (Nano Drop 1000; Thermo Fisher Scientific, Wilmington, DE). The UV absorption of RNA was compared with the spectral sensitivity of RNA measured by RT-qPCR. The ratio of the UV absorption at 260 nm to that at 280 nm was 2.55, confirming the purity of the RNA.

Statistical analysis. For RT-qPCR analyses, serial 10-fold dilution curves were developed to correlate the PCR cross-threshold (C_T) value with the MS2 concentration and measure changes in the log concentrations of gene copies for each fragment. The following linear equation was used for calculating $\log_{10}$ copy numbers when performing RT-qPCR for analysis of the 1,185-base region of the MS2 stock:

$$\log_{10}\text{ copies} = -(0.3244 \times C_T) + 6.9639 \quad r^2 = 0.996 \qquad (1)$$

where r^2 is the coefficient of determination.

For the 2,169-base fragment, the dilution curve was determined as follows:

$$\log_{10}\text{ copies} = -(0.3145 \times C_T) + 12.958 \quad r^2 = 0.981 \qquad (2)$$

The results, which reflected the log reduction for each genome fragment, must be adjusted to apply to the whole genome. Pecson et al. (27) discusses methods for relating genome damage, measured by qPCR, to the loss of MS2 infectivity following exposure to UV light. Those authors introduced a theoretical framework to adjust the results using the ratio of genome size to fragment size. However, different regions of the MS2 genome have different susceptibilities to UV damage (27); therefore, the results were adjusted by using another method proposed in the same publication, by calibrating the qPCR results to empirical infectivity measurements at 253.7 nm (27).

A calibration factor, c, was calculated as the ratio of the lesion rate in each fragment to the lesion rate in the whole genome, as follows:

$$c = \frac{\ln(\text{Proportion}(\text{undamaged genome}))}{\ln(\text{Proportion}(\text{undamaged fragment}))} \qquad (3)$$

The factor c was determined by dividing the ln of damage to the viral genome, estimated for a given dose by using the linear regression from plaque assay infectivity results, by the ln of damage to the fragment, measured by RT-qPCR. Ratios at each point of the dose-response curve at 253.7 nm were averaged to determine the calibration factor for data collected with that fragment. After the calibration factors for each fragment were determined by using the infectivity data at 253.7 nm, they were used with equation 3 at all other wavelengths tested to estimate the ratio of damaged genome (N) to undamaged genome (N_0). The results for 253.7 nm were used as the point of comparison because the action spectrum was taken relative to 253.7 nm.

This analysis assumes single-hit inactivation, in other words, that a single lesion leads to the inactivation of the coliphage and prevents PCR amplification, an assumption that was previously for MS2 (24, 27).

The RT-qPCR results displayed first-order kinetics and no statistically significant curvature. RNA damage was compared to the loss-of-infectivity results reported previously (28), using analysis of covariance (ANCOVA) to statistically compare the linear regressions.

The kinetic constant for the relationship between $\log(C)$ and UV dose was obtained from the regression analysis. The log reduction of MS2 was calculated as

$$\text{log reduction} = \log(C_0) - \log(C) \qquad (4)$$

where $\log(C_0)$ is the log concentration of the unexposed sample obtained from the regression analysis and $\log(C)$ is the measured log concentration.

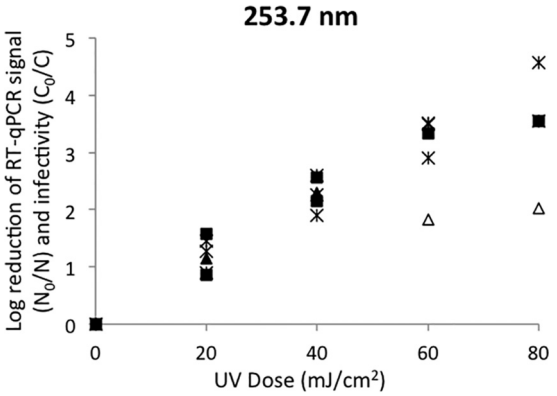

FIG 1 Dose response of MS2 coliphage exposed to UV light from a tunable laser at 253.7 nm as measured by RT-qPCR using two fragments of 1,185 bases (■) and 2,169 bases (▲), after calibration by plaque assay infectivity (×) (28) ($n = 1$). Data represented by open symbols, which indicate that the assay detection limit was reached, were not used for data analysis.

To illustrate the action spectra or spectral sensitivity of the MS2 RNA to UV light, the UV dose-response results at each wavelength tested were mapped to the UV dose response at the reference wavelength of 253.7 nm to obtain a scalar reference value (29). For mapping, the dose-response data obtained by using RT-qPCR with both fragment sizes were fit by using a second-order polynomial equation; mapping constants were defined as $\log I_\lambda = A \times (\alpha_\lambda \times D_\lambda) + B \times (\alpha_\lambda \times D_\lambda)^2$, where $\log I_\lambda$ is the predicted log inactivation, D_λ is the UV dose, λ is the wavelength associated with $\log I_\lambda$ and D_λ, α_λ is the action spectrum constant at wavelength λ, and A and B are constants defining the UV dose response at 253.7 nm. The values of the action spectrum constants were identified as the constants that maximized the R-squared value of the relation between measured $\log I_\lambda$ and D_λ values. The full action spectra were then generated by fitting the averaged values at the wavelength intervals tested with a cubic spline.

RESULTS AND DISCUSSION

The qPCR results were adjusted to reflect UV damage to the entire genome by using equation 3, as described above. The calibration factor, c, values were 2.47 (standard deviation [σ] = 0.12) for the 1,185-base region and 0.98 (σ = 0.06) for the 2,169-base region.

Data for the inactivation of MS2 using the NIST laser at 253.7 nm are presented in Fig. 1. The inactivation rate was 0.050 ($P = 3.6 \times 10^{-7}$) as measured by plaque assay infectivity (28). For the RT-qPCR data points at 253.7 nm calibrated to these infectivity data, the inactivation rates, representing log reductions of qPCR signals, were 0.046 ($P = 6.2 \times 10^{-4}$) for data collected with the 1,185-base region and 0.058 ($P = 1.7 \times 10^{-3}$) for data for the 2,169-base region.

MS2 coliphage consists of a protein capsid surrounding a single-stranded RNA core. Since the coliphage is composed of two primary components, RNA and proteins, the loss of infectivity at a given wavelength must be due to damage to the RNA, damage to the viral proteins, or both. Data for the inactivation of MS2 by the NIST laser at 210 nm, 220 nm, 230 nm, 240 nm, 260 nm, 270 nm, 280 nm, and 290 nm as a function of UV dose are shown in Fig. 2. For initial experiments, the lower operational limit of the laser emission was 212 nm; these data are combined with the results at 210 nm. The results shown represent damage to the full genome, from the log reduction of the RT-qPCR signal measured by using

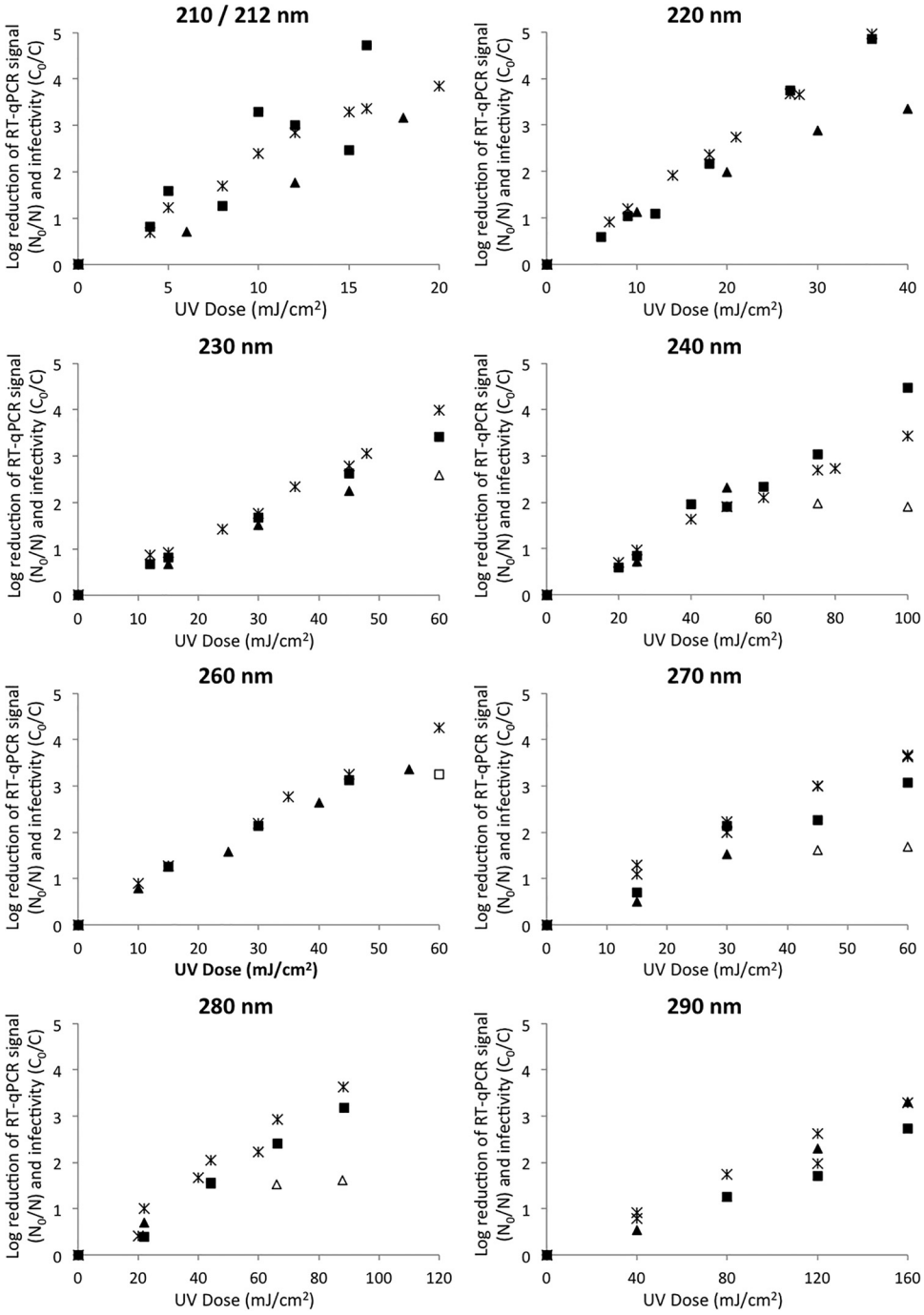

FIG 2 Dose response of MS2 coliphage to monochromatic UV irradiation from a tunable laser. Results represent log reductions of the RT-qPCR signal (N_0/N) measured from two fragments, 1,185 bases (■) and 2,169 bases (▲), compared to the log reduction of MS2 viral infectivity (C_0/C) (×) (28) ($n = 1$). Data represented by open symbols, indicating the assay detection limit, were not used for data analysis. Note the different *x* axis values.

two different fragments, compared with the log reduction of MS2 viral infectivity, reported previously (28). The results indicate that across the germicidal UV spectrum from 210 nm to 290 nm, the rate of damage to the MS2 genome observed closely mirrored the loss of viral infectivity.

PCR is limited because the analyzed regions are susceptible to saturation from multiple photon hits. One lesion prevents the DNA polymerase from carrying out a reaction to transcribe a strand of cDNA. PCR detects only the reduction in transcribed genome fragments; therefore, multiple damage sites are measured as a single point of damage, the log reduction cannot increase, and tailing occurs. In some cases, the assay detection limit for RT-qPCR with the 2,169-base fragment was a 1.5-log reduction. In these cases, no additional damage is quantified, and the UV dose-response curve plateaus. These points, which are represented by open symbols in Fig. 2, were omitted from the regression analysis.

TABLE 2 Wavelength-specific inactivation rate constants, comparing RNA damage (measured with the 1,185-base region) to loss of viral infectivity for MS2 coliphage

Wavelength (nm)	k (cm^2/mJ) (95% CI; P value)		ANCOVA P value[b]
	RNA damage	Infectivity[a]	
210	0.243 (0.1257; 3.2×10^{-3})	0.203 (0.0297; 8.3×10^{-7})	0.421
220	0.141 (0.0180; 5.7×10^{-6})	0.136 (0.0055; 1.1×10^{-10})	0.502
230	0.058 (0.0022; 2.0×10^{-7})	0.065 (0.0044; 4.2×10^{-9})	0.009
240	0.044 (0.0063; 2.5×10^{-6})	0.034 (0.0028; 1.4×10^{-8})	0.002
253.7	0.046 (0.0155; 6.2×10^{-4})	0.050 (0.0095; 3.6×10^{-7})	0.557
260	0.069 (0.0149; 2.6×10^{-3})	0.070 (0.0059; 7.0×10^{-7})	0.739
270	0.051 (0.0216; 4.8×10^{-3})	0.059 (0.0065; 1.2×10^{-7})	0.233
280	0.038 (0.0088; 8.5×10^{-4})	0.043 (0.0075; 8.7×10^{-6})	0.300
290	0.016 (0.0071; 9.9×10^{-3})	0.020 (0.0043; 7.6×10^{-5})	0.214

[a] See reference 28.
[b] For ANCOVA, statistical significance was defined as a P value of <0.05.

Dose-response results for damage to the MS2 viral genome measured by using RT-qPCR with the 1,185-base region best correlated to the dose response of viral infectivity; these results are presented in Table 2. According to ANCOVA, the susceptibility of the MS2 genome to UV light was statistically similar to the susceptibility of the coliphage to UV light emitted at 210 nm, 220 nm, 253.7 nm, 260 nm, 270 nm, 280 nm, and 290 nm. At 230 nm and 240 nm, dose-response results representing RNA damage and viral infectivity were found to be statistically different by ANCOVA. This means that their linear regressions were statistically different, presumably because both data sets had miniscule statistical errors at these wavelengths. However, 95% confidence intervals (CIs) created for the data points overlapped at all wavelengths tested. Regardless, the statistical similarity between the loss of viral infectivity and genome damage at both the low UV wavelengths (<240 nm) and the higher UV wavelengths (>240 nm) suggests that genome damage is the primary mechanism responsible for UV inactivation of MS2 across the germicidal UV spectrum.

Table 3 compares the dose-response data for damage to the MS2 genome measured with the longer region (2,169 bases) with the infectivity results. The results correlated well with infectivity; however, the longer region was unable to detect damage at high UV doses. As described above, higher UV doses generate multiple photon hits in the same base region, which impedes the ability to measure log inactivation. The longer region was more susceptible than the shorter region to photon saturation, which caused many of the linear inactivation curves to plateau, as shown in Fig. 2. Only the linear points were included in calculating the inactivation rate. By ANCOVA, it was shown that the susceptibility of the MS2 genome to UV light was not statistically different ($P < 0.05$) from the susceptibility of the MS2 coliphage at 210 nm, 253.7 nm, 270 nm, 280 nm, and 290 nm. At 220 nm, 230 nm, 240 nm, and 260 nm, the ANCOVA P value target was <0.05, indicating that the linear regressions of genome damage and infectivity were statistically different; however, 95% confidence intervals for both data sets overlapped for all wavelengths tested.

The spectral sensitivities of MS2 and its viral genome relative to their sensitivity at 253.7 nm are given in Fig. 3. The MS2 action spectrum determined by plaque assay infectivity (28) exhibited a relative peak at 260 nm, decreased with UV wavelength to 240 nm, and then increased at wavelengths below 240 nm. This same trend was observed for the spectral sensitivity of the MS2 genome. When measured with either the shorter 1,185-base fragment or the longer 2,169-base fragment, MS2 genome sensitivity also exhibited a relative peak near 260 nm, decreased to 240 nm, and then increased at wavelengths below 240 nm.

The spectral sensitivity of the MS2 genome, when measured with the 1,185-base fragment, did not diverge from the sensitivity of its viral infectivity across the germicidal UV spectrum, and for the 2,169-base fragment, the spectral sensitivity diverged only minimally for a few data points. Based on the data presented in Fig. 3 and statistical analyses, it is apparent that damage to the

TABLE 3 Wavelength-specific inactivation rate constants, comparing RNA damage (measured with the 2,169-base region) to loss of viral infectivity for MS2 coliphage

Wavelength (nm)	k (cm^2/mJ) (95% CI; P value)		ANCOVA P value[b]
	RNA damage	Infectivity[a]	
210	0.176 (0.0780; 0.0104)	0.203 (0.0297; 8.3×10^{-7})	0.232
220	0.085 (0.0203; 9.3×10^{-4})	0.136 (0.0055; 1.1×10^{-10})	4.0×10^{-6}
230	0.051 (0.0064; 8.7×10^{-4})	0.065 (0.0044; 4.2×10^{-9})	1.7×10^{-4}
240	0.046 (0.1278; 0.136)	0.034 (0.0028; 1.4×10^{-8})	0.035
253.7	0.058 (0.0020; 1.7×10^{-3})	0.050 (0.0095; 3.6×10^{-7})	0.515
260	0.061 (0.0079; 1.5×10^{-4})	0.070 (0.0059; 7.0×10^{-7})	0.028
270	0.051 (0.1243; 0.122)	0.059 (0.0065; 1.2×10^{-7})	0.349
280	0.035 (0.0233; 0.033)	0.043 (0.0075; 8.7×10^{-6})	0.353
290	0.021 (0.0052; 1.0×10^{-3})	0.020 (0.0043; 7.6×10^{-5})	0.624

[a] See reference 28.
[b] For ANCOVA, statistical significance was defined as a P value of <0.05.

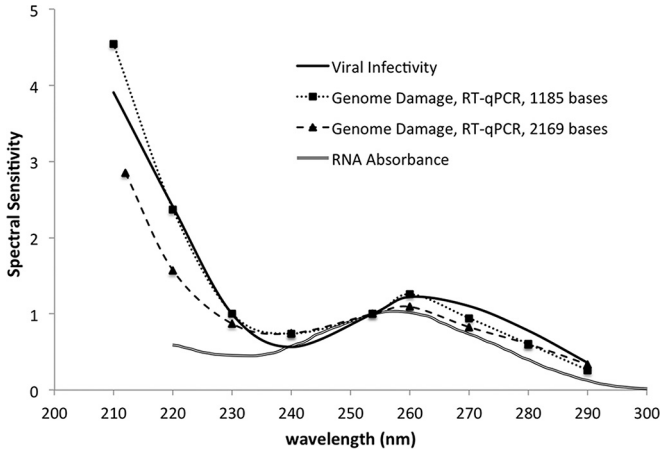

FIG 3 Spectral sensitivity of the MS2 genome (RNA damage measured by RT-qPCR using 1,185- and 2,169-base fragments) and bacteriophage MS2 (measured as viral infectivity [28]) compared to the UV absorption of MS2 RNA at germicidal UV wavelengths.

nucleic acid is the primary cause of the loss of viral infectivity across the germicidal UV spectrum. Although UV light causes photoproducts or structural modifications in capsid proteins (21), and genome-mediated protein damage has been demonstrated in MS2 (30), this damage does not appear to contribute significantly to a loss of MS2 viral infectivity.

In contrast, the spectral sensitivity of adenovirus diverged from the sensitivity of its genome at wavelengths below 240 nm, suggesting that nongenomic damage contributes to UV inactivation at these wavelengths (28). The fact that MS2 coliphage and adenovirus have different mechanisms of UV inactivation at wavelengths below 240 nm is important, particularly since MS2 is used as a surrogate microorganism for virus credit when validating polychromatic UV systems (31). The difference between the mechanisms of inactivation of these two viruses at low UV wavelengths is most likely due to differences in their viral proteins. MS2 infects by attaching its maturation protein to the viral receptor on the F pilus of *E. coli*. The maturation protein exists as a single copy, relative to the 180 copies of coat protein (13). Adenovirus, however, has a more complicated protein structure for infecting human cells. It consists of 13 structural proteins, which play an integral role in the attachment, entry, and release of DNA into the host cell's nucleus (32–34). Therefore, the disinfection of MS2 coliphage using UV irradiation is less enhanced by any nongenomic mechanisms at low wavelengths, contrary to adenovirus disinfection; the use of MS2 as a surrogate for adenovirus would require a correction based on overall action spectrum differences.

Another item of interest regarding the MS2 genome is that the spectral sensitivity of MS2 RNA damage diverges from the UV absorbance of the RNA, with very little absorbance of the RNA being evident at wavelengths below 240 nm. One explanation as to why there would still be genomic damage from irradiation at wavelengths below 240 nm is the potential for proteins absorbing UV at these wavelengths to transfer energy or extend damage to the RNA. Wigginton et al. (30) showed that the presence of viral RNA contributed to site-specific protein damage, suggesting an energy transfer from RNA to viral proteins in MS2 following UV radiation at 253.7 nm. At wavelengths below 240 nm, where protein absorption of UV is highest, it is plausible that the energy transfer would occur in the opposite direction; energy preferentially absorbed by proteins could be generating site-specific RNA damage, resulting in a loss of viral infectivity. Alternatively, damage sustained by the proteins could be extended to the RNA in close proximity, causing RNA-protein cross-links or single-strand breaks. A previous study of the protein association of DNA showed that protein-associated DNA is more susceptible to UV damage than isolated DNA (35). UV-induced RNA-protein cross-linking has been described in the scientific literature (22). For MS2 coliphage, the most abundant protein, the coat protein, binds a stem-loop structure in the viral RNA (13, 36), and the maturation protein is bound to the RNA at two sites, at the 5′ end and the 3′ end (37). At these sites, UV energy could induce a covalent cross-link between the protein and the RNA, or the proteins could transfer the UV energy directly to the RNA, forming a RNA photoproduct. Regardless of the pathways involved, this research shows that inactivation of the RNA bacteriophage MS2 is dominated by damage to the nucleic acids throughout the germicidal wavelength range. Caution should be exercised with the use of nucleic acid absorbance as a proxy for germicidal action.

ACKNOWLEDGMENTS

We thank Kaitlyn Jeanis for her contributions to the RT-qPCR assays. We thank Harold Wright for his leadership in arranging the use of the NIST tunable laser.

This research has not been subjected to any EPA review and therefore does not necessarily reflect the views of the Agency. The mention of certain commercial products in this paper is for information purposes only and does not constitute an endorsement of the product by the authors or their institutions.

FUNDING INFORMATION

National Science Foundation (NSF) under grant number HRD 0639653 and the University of Colorado Boulder SMART program (general fund) jointly funded Michael A. Hawkins. Water Research Foundation (WRF) provided funding to Karl G. Linden under grant number 4376. U.S. Environmental Protection Agency (EPA) provided funding to Sara E. Beck under grant number FP91709801. The funders had no role in study design, data collection and interpretation, or the decision to submit the work for publication.

REFERENCES

1. **Adams RLP, Knowler JT, Leader DP.** 1986. The biochemistry of the nucleic acids, 10th ed. Chapman and Hall, New York, NY.
2. **Cadet J, Anselmino C, Douki T, Voituriez L.** 1992. Photochemistry of nucleic acids. J Photochem Photobiol B Biol **15:**277–298. http://dx.doi.org/10.1016/1011-1344(92)85135-H.
3. **Wellinger RE, Thoma F.** 1996. Taq DNA polymerase blockage at pyrimidine dimers. Nucleic Acids Res **24:**1578–1579. http://dx.doi.org/10.1093/nar/24.8.1578.
4. **Smith CA, Baeten J, Taylor J.** 1998. The ability of a variety of polymerases to synthesize past site-specific cis-syn, trans-syn-II, (6-4), and Dewar photoproducts of thymidylyl-(3′-5′)-thymidine. J Biol Chem **273:**21933–21940. http://dx.doi.org/10.1074/jbc.273.34.21933.
5. **Rosenstein BS, Mitchell DL.** 1987. Action spectrum for the induction of pyrimidine(6-4)pyrimidone photoproducts and cyclobutane pyrimidine dimers in normal human skin fibroblasts. Photochem Photobiol **45:**775–780. http://dx.doi.org/10.1111/j.1751-1097.1987.tb07881.x.
6. **Besaratinia A, Yoon JI, Schroeder C, Bradforth SE, Cockburn M, Pfeifer GP.** 2011. Wavelength dependence of ultraviolet radiation-induced DNA damage as determined by laser irradiation suggests that cyclobutane pyrimidine dimers are the principal DNA lesions produced by terrestrial sunlight. FASEB J **25:**3079–3091. http://dx.doi.org/10.1096/fj.11-187336.
7. **Jagger J.** 1967. Introduction to research in ultra-violet photobiology. Prentice-Hall biological techniques series. Prentice-Hall, Englewood Cliffs, NJ.

8. **Harm W.** 1980. Biological effects of ultraviolet radiation. IUPAB biophysics series 1. Cambridge University Press, Cambridge, England.
9. **Hijnen WAM, Beerendonk EF, Medema GJ.** 2006. Inactivation credit of UV radiation for viruses, bacteria and protozoan (oo)cysts in water: a review. Water Res **40:**3–22. http://dx.doi.org/10.1016/j.watres.2005.10.030.
10. **Linden KG, Thurston J, Schaefer R, Malley JP.** 2007. Enhanced UV inactivation of adenoviruses under polychromatic UV lamps. Appl Environ Microbiol **73:**7571–7574. http://dx.doi.org/10.1128/AEM.01587-07.
11. **Eischeid AC, Linden KG.** 2011. Molecular indications of protein damage in adenoviruses after UV disinfection. Appl Environ Microbiol **77:**1145–1147. http://dx.doi.org/10.1128/AEM.00403-10.
12. **Beck SE, Rodriguez RA, Linden KG, Hargy TM, Larason TC, Wright HB.** 2014. Wavelength dependent UV inactivation and DNA damage of adenovirus as measured by cell culture infectivity and long range quantitative PCR. Environ Sci Technol **48:**591–598. http://dx.doi.org/10.1021/es403850b.
13. **Valegard K, Murray JB, Stonehouse NJ, van den Worm S, Stockley PG, Liljas L.** 1997. The three-dimensional structures of two complexes between recombinant MS2 capsids and RNA operator fragments reveal sequence-specific protein-RNA interactions. J Mol Biol **270:**724–738. http://dx.doi.org/10.1006/jmbi.1997.1144.
14. **Park GW, Linden KG, Sobsey MD.** 2011. Inactivation of murine norovirus, feline calicivirus and echovirus 12 as surrogates for human norovirus (NoV) and coliphage (F+) MS2 by ultraviolet light (254 nm) and the effect of cell association on UV inactivation. Lett Appl Microbiol **52:**162–167. http://dx.doi.org/10.1111/j.1472-765X.2010.02982.x.
15. **Chen RZ, Craik SA, Bolton JR.** 2009. Comparison of the action spectra and relative DNA absorbance spectra of microorganisms: information important for the determination of germicidal fluence (UV dose) in an ultraviolet disinfection of water. Water Res **43:**5087–5096. http://dx.doi.org/10.1016/j.watres.2009.08.032.
16. **Mackey ED, Hargy TM, Wright HB, Malley JP, Cushing RS.** 2002. Comparing Cryptosporidium and MS-2 bioassays—implications for UV reactor validation. J Am Water Works Assoc **94:**62–69.
17. **Maezawa H, Ito T, Hieda K, Kobayashi K, Ito A, Mori T, Suzuki K.** 1984. Action spectra for inactivation of dry phage-T1 after monochromatic (150-254 nm) synchrotron irradiation in the presence and absence of photoreactivation and dark repair. Radiat Res **98:**227–233. http://dx.doi.org/10.2307/3576231.
18. **Mamane-Gravetz H, Linden KG, Cabaj A, Sommer R.** 2005. Spectral sensitivity of Bacillus subtilis spores and MS2 coliphage for validation testing of ultraviolet reactors for water disinfection. Environ Sci Technol **39:**7845–7852. http://dx.doi.org/10.1021/es048446t.
19. **Lakretz A, Ron EZ, Mamane H.** 2010. Biofouling control in water by various UVC wavelengths and doses. Biofouling **26:**257–267. http://dx.doi.org/10.1080/08927010903484154.
20. **Smith KC.** 1963. Photochemical reactions of thymine, uracil, uridine, cytosine and bromouracil in frozen solution and in dried films. Photochem Photobiol **2:**503–517. http://dx.doi.org/10.1111/j.1751-1097.1963.tb08908.x.
21. **Miller RL, Plagemann PGW.** 1974. Effect of ultraviolet light on mengovirus: formation of uracil dimers, instability and degradation of capsid, and covalent linkage of protein to viral RNA. J Virol **13:**729–739.
22. **Wurtmann EJ, Wolin SL.** 2009. RNA under attack: cellular handling of RNA damage. Crit Rev Biochem Mol Biol **44:**34–49. http://dx.doi.org/10.1080/10409230802594043.
23. **Petit-Frere C, Clingen PH, Arlett CF, Green MHL.** 1996. Inhibition of RNA and DNA synthesis in UV-irradiated normal human fibroblasts is correlated with pyrimidine(6-4)pyrimidone photoproducts formation. Mutat Res **354:**87–94.
24. **Simonet J, Gantzer C.** 2006. Inactivation of poliovirus 1 and F-specific RNA phages and degradation of their genomes by UV irradiation at 254 nanometers. Appl Environ Microbiol **72:**7671–7677. http://dx.doi.org/10.1128/AEM.01106-06.
25. **Bolton JR, Linden KG.** 2003. Standardization of methods for fluence (UV dose) determination in bench-scale UV experiments. J Environ Eng **129:**209–215. http://dx.doi.org/10.1061/(ASCE)0733-9372(2003)129:3(209).
26. **Ogorzaly L, Gantzer C.** 2006. Development of real-time RT-PCR methods for specific detection of F-specific RNA bacteriophage genogroups: application to urban raw wastewater. J Virol Methods **138:**131–139. http://dx.doi.org/10.1016/j.jviromet.2006.08.004.
27. **Pecson BM, Ackermann M, Kohn T.** 2011. Framework for using quantitative PCR as a nonculture based method to estimate virus infectivity. Environ Sci Technol **45:**2257–2263. http://dx.doi.org/10.1021/es103488e.
28. **Beck SE, Wright HB, Hargy TM, Larason TC, Linden KG.** 2015. Action spectra for validation of pathogen disinfection in medium-pressure ultraviolet (UV) systems. Water Res **70:**27–37. http://dx.doi.org/10.1016/j.watres.2014.11.028.
29. **Sutherland JC.** 2002. Biological effects of polychromatic light. Photochem Photobiol **76:**164–170. http://dx.doi.org/10.1562/0031-8655(2002)076<0164:BEOPL>2.0.CO;2.
30. **Wigginton KR, Menin L, Sigstam T, Gannon G, Cascella M, Hamidane HB, Tsybin YO, Waridel P, Kohn T.** 2012. UV radiation induces genome-mediated, site-specific cleavage in viral proteins. Chembiochem **13:**837–845. http://dx.doi.org/10.1002/cbic.201100601.
31. **Linden KG, Wright HB, Collins J, Cotton C, Beck SE.** 2015. Guidance for implementing action spectra correction factors with medium pressure UV disinfection. American Public Health Association, Washington, DC.
32. **Wickham TJ, Mathias P, Cheresh DA, Nemerow GR.** 1993. Integrins alpha v beta 3 and alpha v beta 5 promote adenovirus internalization but not virus attachment. Cell **73:**309–319. http://dx.doi.org/10.1016/0092-8674(93)90231-E.
33. **Seth P.** 1999. Adenoviruses: basic biology to gene therapy, p 31–38. RG Landes Company, Austin, TX.
34. **Russell WC.** 2009. Adenoviruses: update on structure and function. J Gen Virol **90:**1–20. http://dx.doi.org/10.1099/vir.0.003087-0.
35. **Hegedus M, Modos K, Ronto G, Fekete A.** 2003. Validation of phage T7 biological dosimeter by quantitative polymerase chain reaction using short and long segments of phage T7 DNA. Photochem Photobiol **78:**213–219. http://dx.doi.org/10.1562/0031-8655(2003)078<0213:VOPTBD>2.0.CO;2.
36. **Peabody DS.** 1993. The RNA binding site of bacteriophage MS2 coat protein. EMBO J **12:**595–600.
37. **Shiba T, Suzuki Y.** 1981. Localization of A protein in the RNA-A protein complex of RNA phage MS2. Biochim Biophys Acta **654:**249–255. http://dx.doi.org/10.1016/0005-2787(81)90179-9.